SEGREGATION-DRIVEN ASSEMBLY OF GRAPHITE FLUORIDE USING POLYMETHYL METHACRYLATE BEADS FOR ENHANCED THERMAL CONDUCTIVITY IN FLEXIBLE PDMS COMPOSITES

Mai Thi Kieu Lien[1]*, Nguyen Thi My Duc[1], Tran Thi Hong[1], Trinh Ngoc Dat[1], Nguyen Thanh Son[2], Nguyen Thanh Hoi[3], Le Hong Nam[4], Tran Thi Thu Hien[5]

[1]The University of Danang - University of Science and Education, Vietnam
[2]The University of Danang - Advanced Institute of Science and Technology, Vietnam
[3]The University of Danang - Center for Continuing Education, Vietnam
[4]The University of Danang - University of Science and Technology, Vietnam
[5]Hung Vuong Secondary School, Phan Thiet, Binh Thuan, Vietnam

*Corresponding author: mtklien@ued.udn.vn

(Received: April 19, 2025; Revised: May 20, 2025; Accepted: June 06, 2025)

DOI: 10.31130/ud-jst.2025.23(6A).219E

Abstract - Flexible thermal interface materials are crucial for soft electronics, yet enhancing thermal conductivity without sacrificing mechanical compliance remains challenging. Herein, we present a facile approach to improve heat dissipation in Ecoflex elastomers by inducing graphite fluoride (GF) segregation using polymethyl methacrylate (PMMA) beads as spatial templates. Composites were fabricated with varying PMMA bead sizes (5–50 μm) and GF loadings (10–20 wt%) to optimize filler network morphology and thermomechanical properties. Scanning electron microscopy revealed that 25 μm beads effectively promoted GF segregation into continuous domains. As a result, thermal conductivity reached up to 9.23 W/mK at 20 wt% GF. Real-device testing with surface-mounted LEDs demonstrated superior heat dissipation, significantly reducing steady-state temperatures. This study highlights the effectiveness of bead-induced segregation in engineering soft, thermally conductive composites. The resulting materials offer a promising solution for wearable electronics, flexible displays, and soft robotics where mechanical flexibility and thermal performance must be simultaneously achieved.

Key words - Graphite fluoride; thermal conductivity; flexible polymer composites; PDMS; PMMA beads

1. Introduction

The emergence of flexible and wearable electronic devices has sparked a significant transformation in the design of energy management systems, particularly in thermal regulation components. Flexible substrates have become foundational in next-generation devices such as foldable phones, wearable biosensors, and implantable medical electronics. Despite their growing functionality and integration complexity, thermal management remains a limiting factor in achieving high performance and long-term stability [1]. As device dimensions shrink and power densities increase, efficient heat dissipation becomes indispensable to prevent local overheating, degradation of active layers, and performance fluctuations over time[2].

Traditional thermal interface materials, particularly those based on rigid thermally conductive ceramics or metals, fail to conform to the mechanical compliance and bending resilience required by flexible systems[3]. These rigid materials, including aluminum oxide and boron nitride composites embedded in epoxy, exhibit high thermal conductivity but suffer from mechanical brittleness, processing challenges, and poor integration with elastomeric substrates[4], [5]. This has motivated a research shift toward the development of flexible and soft thermal conductive composites (FTCCs) that offer both heat dissipation efficiency and mechanical adaptability.

Polymers such as polydimethylsiloxane (PDMS), polyurethane (PU), and polyvinylidene fluoride (PVDF) have gained attention due to their softness, ease of processing, biocompatibility, and resilience to cyclic mechanical stress. However, their intrinsically low thermal conductivities, typically in the range of 0.1–0.3 W/mK, severely limit their utility in heat-dissipating applications [6]. To overcome this limitation, researchers have embedded high thermal conductivity fillers into polymer matrices. Common fillers include carbon-based materials (e.g., graphite, graphene, and carbon nanotubes), metal nanoparticles, and ceramic particles (e.g., AlN, BN, SiC) [7]. While these fillers significantly improve the composite's thermal conductivity, the challenge of achieving high conductivity at low filler loadings without sacrificing flexibility, transparency, or processability remains unresolved [8] - [10].

Recent literature has highlighted several strategies to optimize the thermal performance of polymer composites. These include modifying filler geometry, surface functionalization, alignment techniques, and constructing percolation networks [11] - [13]. For example, thermally conductive pathways can be constructed by aligning high-aspect-ratio fillers such as graphene sheets or carbon nanotubes within a polymeric matrix, allowing phonons to travel more efficiently across the network [14], [15]. Such strategies have yielded in-plane thermal conductivity values surpassing 10 W/mK at moderate filler concentrations.

More sophisticated techniques involve the use of segregated network structures, where thermally conductive fillers are confined to interfacial regions rather than uniformly dispersed throughout the polymer. These segregated structures enable efficient phonon transport at lower filler volume fractions, mitigating the trade-off

between thermal conductivity and mechanical softness. For instance, the use of polymer particles such as PMMA (polymethyl methacrylate) as space-occupying templates during composite formation has been reported to drive filler segregation due to volume exclusion effects [5], [16], [17]. Upon annealing or solvent removal, these sacrificial beads induce a morphology in which fillers are clustered into continuous conductive domains, facilitating thermal transport.

Another promising pathway involves the application of elastomeric matrices such as silicone matrix, which offers excellent thermal and mechanical stability, elasticity, and compatibility with microfabrication techniques. Silicone-based composites have been fabricated using 3D printing, phase separation, and templating methods to introduce porosity or enable selective filler deposition. In recent [18]studies, liquid metal/Ecoflex composites showed high stretchability (up to 400% fracture strain) and thermal conductivity up to 9.8 W/mK indicating their dual applicability in both thermal and mechanical domains. However, liquid metal/Ecoflex composites possess high electrical conductivity, which may lead to electrical short circuits, thereby limiting their use in electronic devices that demand simultaneous thermal conductivity and electrical insulation.

Graphite fluoride (GF) is a highly fluorinated form of graphite that possesses a unique combination of low surface energy, chemical stability, and relatively high intrinsic thermal conductivity and electrical insulation [19]. Unlike pure graphite, GF demonstrates improved oxidation resistance and can participate in hydrogen bonding due to the presence of –CF groups. Its layered structure offers in-plane thermal conductivity pathways, and its chemical tunability makes it compatible with polymer matrices. However, similar to other 2D fillers, the thermal conductivity enhancement from GF depends critically on its dispersion and spatial distribution within the host polymer [1], [19].

In conventional dispersion approaches, GF tends to aggregate due to strong van der Waals interactions, leading to heterogeneous domains and impaired phonon transport. To overcome this, volume exclusion strategies can be employed using polymer beads such as PMMA. PMMA beads, when incorporated into an Ecoflex precursor mixed with GF, occupy discrete volumes that restrict filler dispersion into the matrix bulk. As a result, GF is preferentially expelled toward the inter-bead regions or Ecoflex interfaces, forming a segregated network upon bead removal or polymer curing. This mechanism parallels the “island-bridge” morphology observed in conductive composites, where polymer microspheres template the assembly of fillers at their boundaries (Figure 1b-c).

This work proposes a novel strategy for enhancing the thermal conductivity of flexible Ecoflex composites through the spatial segregation of GF fillers induced by PMMA bead templates. The hypothesis is that the introduction of PMMA beads leads to a phase-separated structure during composite formation, where GF is expelled into narrow interfacial regions, forming a percolative heat-conducting network. Upon curing, the resulting composite exhibits a pronounced enhancement in thermal conductivity compared to homogeneously mixed systems (Figure 1a). This study systematically investigates the influence of PMMA bead size, graphite loading fraction, and distribution on the segregation behavior of GF within the Ecoflex matrix (Figure 1b-c). The resulting composite microstructures are characterized using SEM, thermal conductivity is measured using laser flash analysis, and mechanical flexibility is evaluated under tensile test. This research provides a pathway for scalable, low-cost fabrication of thermally conductive elastomers suitable for wearable electronics, soft robotics, and conformal heat spreaders in advanced thermal management systems.

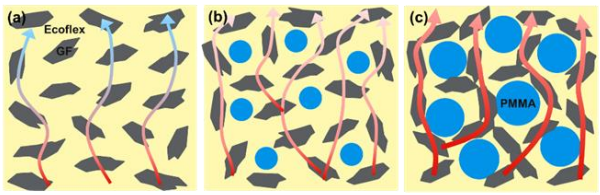

Figure 1. *Illustration of segregation effect influence on heat transfer in composites (a) GF randomly dispersed in Ecoflex matrix, (b) GF and small size of PMMA bead randomly dispersed in Ecoflex matrix, (c) GF and large size of PMMA bead randomly dispersed in Ecoflex matrix*

2. Experimental Section

2.1. Materials

Silicone polymer (Ecoflex base and curing agent) was obtained from SmoothOn and used as the elastomer matrix without further purification. GF powder with an average particle size of approximately 5 µm and a fluorination degree greater than 60% was purchased from Sigma-Aldrich. Polymethyl methacrylate (PMMA) microspheres with nominal particle sizes of 5 µm, 25 µm, and 50 µm were procured from MicroParticles GmbH and served as sacrificial templates to induce filler segregation via volume exclusion. All reagents were used as received.

2.2. Fabrication of Gx-Py/PDMS composites

Two groups of Ecoflex composites containing GF and PMMA beads (Gx-Py/Eco composites) were prepared to study the effects of PMMA bead size and GF loading on filler segregation and composite properties. In the first group, the GF content was fixed at 10 wt% while the PMMA content was maintained at 10 wt%, with bead sizes varied between 5 µm, 25 µm, and 50 µm. In the second group, the PMMA content was fixed at 10 wt% with 25 µm bead size, and the GF content was varied at 10 wt%, 15 wt%, and 20 wt%. All compositions were shown in Table 1.

For composite fabrication, predetermined amounts of GF and PMMA beads were first premixed in a dry state using a mortar and pestle. The powder mixture was then added to the Ecoflex precursor solution, prepared by mixing the base and curing agent at a 10:1 weight ratio. The composite mixture was manually stirred, followed by planetary centrifugal mixing (Thinky ARE-310) at 2000 rpm for 2 min to ensure homogeneous dispersion of fillers. The resulting slurry was poured into

polytetrafluoroethylene (PTFE) molds and degassed under vacuum for 30 min to remove entrapped air. Curing was carried out in an oven at 80°C for 2 h. The final samples were cut into appropriate dimensions for further characterization.

Table 1. *Gx-Py/Eco composite compositions.*

Composites	PMMA size (μm)	PMMA content (wt%)	GF content (wt%)	PDMS (wt%)
G10-P5/Eco	5	10	10	80
G10-P25/Eco	25	10	10	80
G10-P50/Eco	50	10	10	80
G15-P25/Eco	25	10	15	75
G20-P25/Eco	25	10	20	70

2.3. Characterization

2.3.1. Morphology

The internal microstructure and spatial distribution of GF were examined using scanning electron microscopy (SEM, JEOL JSM-IT 200). Samples were cryo-fractured in liquid nitrogen to obtain clean cross-sections and then sputter-coated with platinum to prevent charging. Morphological analysis focused on identifying the degree of GF segregation and the connectivity of the percolative network as influenced by PMMA size and GF content.

2.3.2. Mechanical testing

Tensile properties were measured using a universal testing machine (Instron 5567). Rectangular-shaped specimens (gauge length: 20 mm; width: 4 mm; thickness: 2 mm) were tested at a crosshead speed of 50 mm/min. The tensile strength, Young's modulus, and elongation at break were extracted from stress–strain curves. Each measurement was performed on at least three specimens to ensure statistical reliability.

2.3.3. Thermal conductivity measurement

Thermal conductivity was evaluated using the laser flash analysis method (Netzsch LFA 467). Disc-shaped specimens with a diameter of 12.7 mm and a thickness of ~2 mm were used. Thermal diffusivity (α) was measured, and thermal conductivity (k) was calculated by:

$$k=\alpha\cdot\rho\cdot C \quad (1)$$

where ρ is the bulk density measured by the Archimedes method, and C is the specific heat capacity of Ecoflex, taken as 1.46 J/gK. All measurements were carried out at room temperature. To ensure statistical reliability, all thermal conductivity measurements were conducted in triplicate for each sample.

2.3.4. Heat dissipation performance

To assess practical heat dissipation capabilities, a commercial 50 W LED chip was mounted on the surface of each composite sample (25 mm × 25 mm × 2 mm) using thermal paste to ensure good thermal contact. The LED was powered continuously using a DC power supply (9 V, 300 mA), and the surface temperature was monitored over time using an infrared (IR) thermal imaging camera (FLIR E6-XT). The maximum surface temperature at steady state was recorded and compared among all samples. Lower equilibrium temperatures were indicative of improved thermal conductivity and heat-spreading efficiency.

3. Results

3.1. Morphology

The morphology of G*x*-P*y*/Eco composites was investigated by SEM to examine the effect of PMMA bead size and GF loading on the development of segregated filler networks. Figure 2a shows the smooth surface of the Ecoflex matrix (without adding fillers). In the G10-P5/Eco composite, Figure 2b images revealed that GF was relatively uniformly dispersed throughout the Ecoflex matrix, with minimal localization at inter-bead regions. The 5 μm PMMA beads resulted in narrow interstitial gaps, which limited the spatial confinement required for effective volume exclusion. Consequently, the GF particles remained distributed across the matrix rather than being effectively expelled into continuously segregated domains. The filler appeared discontinuous and poorly interconnected, lacking a long-range percolated structure. The G10-P25/Eco sample (Figure 2c), in contrast, showed a significant change in GF distribution. In this formulation, GF particles were largely expelled from the PMMA-rich domains and accumulated along the bead interfaces. The interstitial regions between 25 μm PMMA beads were densely populated with GF, forming continuous and interconnected conductive paths. The geometry of the beads provided sufficient volume displacement and spacing to accommodate GF segregation while maintaining a high degree of inter-bead contact, promoting the formation of extended networks suitable for thermal conduction. The morphology observed in this sample indicates an optimal volume exclusion effect induced by the 25 μm PMMA template size. In the G10-P50/Eco composite (Figure 2d), although GF segregation along PMMA bead interfaces was still evident, the structure appeared more fragmented. The increased PMMA bead size reduced the number of inter-bead contact points per unit volume, leading to longer diffusion distances for GF particles and larger gaps between filler domains. As a result, the connectivity between segregated GF zones diminished, and the percolation network appeared less uniform. Moreover, the increased size of the interstitial regions led to uneven GF accumulation and localized discontinuities in the conductive framework.

To further evaluate the role of GF concentration on segregation behavior, SEM analysis was carried out on composites with increasing GF content at constant PMMA parameters (25 μm, 10 wt%). In the G15-P25/Eco sample (Figure 2e), the interstitial zones were more densely filled with GF compared to G10-P25/Eco. The segregated network exhibited greater continuity and more uniform filler coverage along the PMMA bead boundaries. GF domains were broader and more extensively overlapped, forming robust percolating structures with reduced inter-domain voids. The increased filler concentration facilitated enhanced particle-particle contact within the segregated regions, which is expected to improve thermal transport properties. In the G20-P25/Eco formulation (Figure 2e), GF accumulation within the inter-bead spaces became even

more prominent. The filler formed thick, overlapping layers along PMMA interfaces, and in some areas, dense agglomerates were observed. While the network appeared continuous, excessive GF content resulted in local filler clustering and non-uniform packing. These agglomerated domains may act as phonon scattering sites, and the risk of interfacial delamination or stress concentration increases due to compromised dispersion homogeneity. The dense and heavily loaded GF structure, although beneficial to thermal conductivity, may impose limitations on mechanical flexibility and structural uniformity.

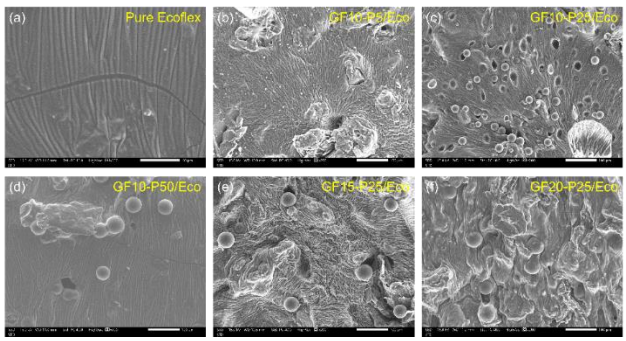

Figure 2. *SEM images of (a) pristine Ecoflex matrix, (b) GF10-P5/Eco, (c) GF10-P25/Eco, (d) GF10-P50/Eco, (e) GF15-P25/Eco, and (f) GF20-P25/Eco composites, respectively*

3.2. Mechanical properties

In addition to thermal conductivity, mechanical performance is a critical design criterion for polymer composites, particularly in applications involving soft robotics, wearable electronics, and stretchable energy devices[20]. These applications demand materials that can simultaneously offer high thermal transport capabilities and mechanical compliance under deformation. To assess the impact of GF content and filler morphology on mechanical flexibility, tensile tests were conducted on all composite formulations. The key mechanical parameters evaluated included tensile strength, elongation at break, and Young's modulus. These values were derived from stress–strain curves obtained in accordance with ASTM D412 using dog-bone-shaped specimens tested under uniaxial tension at a constant strain rate of 50 mm/min. Stress-strain curves of the Ecoflex composites were presented in Figure 3a.

Pristine Ecoflex, known for its outstanding stretchability and softness, exhibited a tensile strength of approximately 0.75 MPa, a Young's modulus of 0.15 MPa, and an elongation at break exceeding 500%. These values serve as a baseline reference, representing the upper limit of ductility and the lower bound of stiffness in the system. Upon the introduction of 10 wt% GF and 10 wt% PMMA beads, significant changes in mechanical behavior were observed, with trends varying across both bead size and GF content.

In the PMMA bead size series (Figure 3b), the G10-P5/Eco sample displayed the highest elongation at break among the composites (~230%) but the lowest tensile strength (0.54 MPa) and modulus (0.21 MPa). The relatively homogeneous distribution of GF within the matrix, due to the ineffective volume exclusion caused by the small 5 μm PMMA beads, allowed the composite to deform more uniformly under tensile load. However, the absence of a reinforced segregated network limited its ability to transfer stress efficiently, resulting in premature yielding and low stiffness. This formulation retained much of the elastomeric character of pure Ecoflex but lacked significant structural reinforcement from the fillers.

The G10-P25/Eco composite exhibited the most balanced mechanical properties, with a tensile strength of 0.62 MPa, a Young's modulus of 0.26 MPa, and an elongation at break of approximately 210%. The optimized microstructure formed by the 25 μm PMMA beads facilitated the development of well-connected, yet evenly dispersed GF domains. These networks acted as reinforcing microstructures that bore part of the applied stress and improved mechanical resilience without drastically compromising flexibility. The integrity of the Ecoflex matrix was largely preserved, and the well-distributed stress transfer across the GF framework helped prevent localized fracture initiation. The moderate enhancement in stiffness, combined with high stretchability, makes G10-P25/Eco particularly suitable for thermal interface applications where moderate mechanical loading is expected.

In contrast, the G10-P50/Eco formulation showed a further reduction in elongation at break (~180%) and tensile strength (0.48 MPa), while Young's modulus increased slightly to 0.29 MPa. The large PMMA beads (50 μm) generated coarse GF domains that were only partially interconnected, leading to poor dispersion uniformity and stress localization under strain. SEM images showed isolated GF-rich regions separated by large Ecoflex pockets, which likely acted as mechanical discontinuities. Under tensile loading, these weak points facilitated crack initiation and propagation, ultimately reducing the material's ductility and toughness. While increased modulus typically correlates with improved thermal pathways, the accompanying reduction in elongation highlights the importance of structural homogeneity in maintaining mechanical performance.

The influence of GF content was further explored in the GF loading series, where the PMMA bead size and content were held constant (25 μm, 10 wt%), as shown in Figure 3c. In this series, mechanical performance followed an inverse trend with thermal conductivity. The G15-P25/Eco composite showed a moderate increase in modulus (0.33 MPa) and tensile strength (0.67 MPa), while elongation decreased to ~170%. The densification of the GF network improved the stiffness and load-bearing capacity of the composite, enabling it to resist deformation more effectively. However, the reduced volume of the elastomer matrix and the increased interfacial area between rigid filler and soft polymer inevitably restrict chain mobility, leading to a moderate decrease in stretchability. Nevertheless, G15-P25/Eco maintained a desirable balance between mechanical robustness and flexibility, suggesting its suitability for thermomechanical coupling applications.

At the highest filler loading of 20 wt% GF, the G20-P25/Eco composite showed the greatest modulus increase (0.45 MPa) but suffered a significant loss in ductility, with

elongation at break dropping to ~120%. The tensile strength remained stable at ~0.64 MPa, suggesting that the load-bearing capacity was not further improved despite the increased filler concentration. The pronounced reduction in elongation is likely due to the onset of filler agglomeration observed in SEM images. These dense GF clusters disrupted the uniform stress field during tensile deformation, acting as rigid inclusions that initiated microcrack formation at lower strain thresholds. Additionally, the reduced continuity of the elastomer phase hindered load distribution, amplifying local strain and causing premature failure.

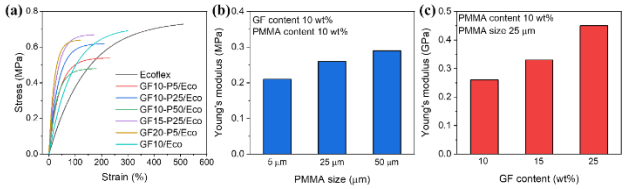

Figure 3. *(a) Stress-strain curves, (b-c) Young's modulus of Ecoflex composites.*

3.3. Thermal conductivity

Thermal conductivity is a key functional parameter in polymer composites designed for thermal interface applications, particularly in soft and flexible electronics. The primary goal of this study was to significantly enhance the thermal conductivity of Ecoflex elastomers while retaining their mechanical compliance by employing a segregated GF network formed via PMMA-induced volume exclusion.

The thermal conductivity of GF/Ecoflex composites increased significantly with rising GF content, demonstrating the strong influence of thermally conductive filler concentration on heat transport in elastomeric matrices (Figure 4a). Pristine Ecoflex exhibited a baseline thermal conductivity of 0.19 W/mK, consistent with its soft, amorphous silicone structure and low intrinsic thermal conductivity. Upon the incorporation of 10 wt% GF, the thermal conductivity increased markedly to 1.01 W/mK, indicating the establishment of initial conductive pathways. Further increasing the GF content to 15 wt% led to a substantial rise in thermal conductivity to 2.32 W/mK, while at 20 wt%, the composite achieved a maximum value of 3.66 W/mK. This trend highlights the formation and densification of thermally conductive networks as GF content increases, allowing for more efficient phonon transport through the matrix. The nonlinear growth in thermal conductivity suggests a percolation-like behavior, where a threshold between 10 and 15 wt% GF enables a transition from isolated filler particles to continuous thermal pathways. These results clearly demonstrate the potential of GF as an effective additive for enhancing thermal conductivity in flexible silicone-based composites, even in the absence of filler alignment or structuring techniques.

To explore the influence of PMMA-induced segregation on the thermal conductivity of Ecoflex composites, a series of samples containing 10 wt% GF and 10 wt% PMMA beads of varying sizes (5 μm, 25 μm, and 50 μm) were prepared, while keeping the matrix and processing conditions constant (Figure 4b). The goal was to assess how the geometry of the sacrificial PMMA template impacts the redistribution of GF fillers within the matrix and how that, in turn, affects the formation of thermally conductive networks.

The addition of GF and PMMA introduced both thermally conductive filler and a mechanism for its spatial redistribution. Upon incorporating 5 μm PMMA beads (G10-P5/Eco), the thermal conductivity increased to 1.85 W/mK. The moderate improvement indicates that while some filler aggregation may have occurred during curing, the small bead size resulted in minimal volume exclusion. Consequently, GF particles were not significantly displaced into continuous inter-bead domains, but instead remained relatively dispersed throughout the matrix. This hindered the formation of long-range conductive pathways, leading to increased phonon scattering across polymer-rich gaps. Additionally, the high packing density of 5 μm beads created narrow and tortuous channels, making it difficult for GF to align or percolate efficiently.

In contrast, the composite containing 25 μm PMMA beads (G10-P25/Eco) exhibited a significantly higher thermal conductivity of 2.99 W/mK. This nearly 60% increase over the 5 μm counterpart illustrates the enhanced filler organization enabled by intermediate-sized beads. The 25 μm PMMA particles generated sufficient interstitial volume to allow GF particles to be effectively excluded during the mixing process. These particles were confined into well-defined regions between the beads, facilitating the formation of continuous GF-rich domains. Moreover, the inter-bead distances at this size scale were sufficiently short to promote inter-domain connectivity, while still spacious enough to permit filler mobility and alignment. This combination resulted in a highly interconnected percolation network, which is critical for promoting efficient phonon transport through the composite. The superior thermal conductivity in G10-P25/Eco indicates that 25 μm represents a geometrically favorable condition for balancing bead spacing, filler confinement, and network overlap.

The most pronounced enhancement was observed in the G10-P50/Eco composite, in which PMMA beads with a diameter of 50 μm were used. This sample exhibited a thermal conductivity of 4.34 W/mK more than 22-fold higher than that of pure Ecoflex. The large PMMA beads created wide interstitial regions, encouraging the extensive accumulation and clustering of GF particles. This confinement allowed for the formation of thick, continuous thermally conductive domains with minimal polymer interruptions. The broader and more densely populated filler pathways reduced interfacial thermal resistance and increased the effective thermal conduction cross-section. Furthermore, the lower number density of 50 μm beads compared to 5 μm or 25 μm beads minimized the total number of interfaces and potential defect sites, which could otherwise disrupt phonon propagation.

However, it is important to note that while G10-P50/Eco yielded the highest thermal conductivity, excessively large PMMA beads can also introduce

challenges. The wider inter-bead distances may increase the risk of GF agglomeration, leading to structural heterogeneity and possible mechanical compromise. In addition, fewer inter-bead contact points may reduce redundancy in conductive paths, making the network more sensitive to local defects or filler misalignment. Despite these concerns, the thermal performance data clearly show that larger PMMA beads up to 50 µm in this study are highly effective in facilitating the segregation and network formation of GF.

To further understand the relationship between filler loading and thermophysical properties, the thermal conductivity of GF/P25/Eco composites was evaluated as a function of GF content while keeping the PMMA bead size and content constant at 25 µm and 10 wt%, respectively. The resulting thermal conductivity values showed a steep, nonlinear increase with increasing GF content, demonstrating the pronounced impact of segregation-induced filler structuring on phonon transport within the composite system (Figure 4c).

At a GF content of 10 wt% (G10-P25/Eco), the thermal conductivity reached 2.29 W/mK, already representing a more than 12-fold enhancement compared to neat Ecoflex (0.19 W/mK). This significant improvement at relatively low filler loading can be attributed to the efficient segregation of GF into interstitial regions between PMMA beads, forming continuous, interconnected thermally conductive domains. The spatial confinement introduced by the PMMA spheres forces the GF particles to accumulate along bead interfaces, minimizing polymer-rich zones and enhancing filler–filler contact. As a result, long-range percolated networks are established even at moderate GF loading, allowing heat to travel efficiently across the composite.

When the GF content was increased to 15 wt% (G15-P25/Eco), the thermal conductivity exhibited a sharp rise to 5.21 W/mK. This marked increase indicates a densification of the existing segregated network. The interstitial regions between PMMA beads became more densely packed with GF particles, resulting in thicker conduction channels, shorter thermal resistive gaps, and more robust filler connectivity. The addition of more GF at this stage amplifies the number of phonon-conducting pathways and increases the effective cross-sectional area available for thermal transport. Moreover, the uniformity of the segregated network at 15 wt% GF is maintained, as the filler concentration remains within the optimal range for ordered packing without introducing significant agglomeration. The dramatic increase in thermal conductivity from 2.99 W/mK to 5.21 W/mK between 10 and 15 wt% suggests that the system reaches or surpasses the thermal percolation threshold in this interval. This is a critical point where isolated filler domains begin to coalesce into a fully interconnected framework, allowing phonons to propagate with minimal scattering losses.

At 20 wt% GF (G20-P25/Eco), the thermal conductivity reached a maximum value of 9.23 W/mK. This continued improvement is attributed to the near-complete saturation of interstitial spaces with GF, further reducing the presence of insulating polymer regions and maximizing the density of the conductive network. However, SEM analysis at this loading typically reveals early signs of filler agglomeration and network coarsening. While these agglomerates may continue to enhance thermal conductivity due to increased local filler density, they can also introduce morphological non-uniformity and localized phonon scattering. The diminishing slope of thermal conductivity increase beyond 15 wt% GF suggests that the system approaches a plateau region, where additional filler contributes marginal gains due to reduced network refinement or excess packing beyond percolation saturation.

The observed trend from 4.87 W/mK at 10 wt% GF to 9.23 W/mK at 20 wt% GF confirms that the combination of template-directed segregation and strategic filler concentration enables the formation of highly effective thermally conductive networks in soft elastomers. Compared to composites with randomly dispersed fillers, where much higher filler loadings are typically required to achieve similar conductivities, the segregated architecture in GF/P25/Eco composites provides an efficient and scalable route to maximize thermal performance with minimal material consumption. This not only benefits processing and cost-efficiency but also ensures that the mechanical softness and flexibility of the Ecoflex matrix are better preserved compared to non-segregated systems.

Stability tests were performed on the composite samples subjected to 500 stretch-release cycles at a 50% strain. After cycling, thermal conductivity was re-evaluated. The results showed less than 10% variation compared to the initial values, indicating excellent structural integrity and thermal transport stability under repeated mechanical deformation.

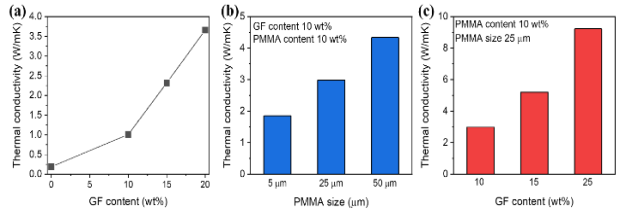

Figure 4. *Thermal conductivity of (a) Ecoflex composites as a function of GF content without PMMA beads, (b) GF10-Py/Eco composites as a function of PMMA bead size, (c) GFx-P25/Eco composites as a function of GF content.*

3.4. LED heat dissipation

To evaluate the practical thermal management capability of the developed composites, a comparative study was performed using a high-power 50 W LED chip operated continuously under simulated conditions. The surface temperature of the LED mounted on different thermal interface materials (TIMs) was recorded after 10 minutes of operation using an infrared (IR) thermal camera. The tested materials included a commercial thermal pad (1.5 W/mK), unstructured GF10/Ecoflex (without PMMA), and segregated GF/Ecoflex composites fabricated using 5 µm, 25 µm, and 50 µm PMMA beads (denoted as GF10-P5/Eco, GF10-P25/Eco, GF10-P50/Eco, respectively), along with the higher GF-loaded composite GF20-P25/Eco. All

samples were dimensionally consistent (25 mm × 25 mm × 2 mm) and mounted using a uniform layer of thermal paste to ensure consistent interface resistance.

The commercial thermal pad exhibited the highest LED surface temperature of 99.0°C, reflecting its limited capacity to dissipate heat from the LED junction. Despite its claimed thermal conductivity of 1.5 W/mK, the commercial pad's performance was likely influenced by interfacial imperfections, compressibility mismatch, or inadequate filler connectivity. This result served as a baseline against which the performance of the experimental Ecoflex-based composites could be assessed.

The composite containing 10 wt% GF without PMMA structuring (GF10/Eco) slightly improved LED cooling, with a recorded surface temperature of 98.7 °C. The marginal reduction suggests that, while the inclusion of thermally conductive fillers enhances bulk conductivity to some extent, the absence of spatial filler organization limits the formation of efficient conduction pathways. In this randomly dispersed system, the GF particles were not aligned or concentrated into percolated domains, leading to discontinuous thermal channels and a high degree of phonon scattering. Consequently, the conductive benefit of the filler was not fully translated into system-level thermal performance.

In contrast, all three segregated composites demonstrated progressively enhanced heat dissipation performance as PMMA bead size increased. The LED temperature recorded on GF10-P5/Eco was 97.3 °C, a reduction of 1.4 °C relative to the unstructured GF10/Eco. This improvement, although modest, indicates the early-stage formation of segregated networks within the Ecoflex matrix. The 5 µm PMMA beads began to induce partial filler displacement into interstitial zones, facilitating more localized GF clustering. However, the small inter-bead distances likely restricted extensive network formation, and the high density of PMMA domains may have hindered continuous percolation.

When the PMMA bead size was increased to 25 µm (GF10-P25/Eco), the LED surface temperature decreased further to 97.0 °C. This enhancement is consistent with the improved thermal conductivity of this formulation, previously measured at 2.99 W/mK. The 25 µm PMMA beads enabled a more effective volume exclusion effect, driving GF particles into well-defined, interconnected domains between beads. The resulting segregated network allowed phonons to traverse longer distances with fewer interruptions, improving heat transfer from the LED base to the underlying composite.

The GF10-P50/Eco composite yielded an even lower LED temperature of 96.6 °C. The larger 50 µm PMMA beads created wide inter-bead channels that accommodated dense GF accumulations and thick thermal pathways. The decreased interfacial resistance and larger conduction cross-sections led to enhanced heat-spreading efficiency. While SEM analysis of this formulation showed a slight decline in network uniformity compared to GF10-P25/Eco, the overall conductive framework remained sufficiently intact to outperform the smaller bead variants. The progressive drop in LED temperature from GF10/Eco to GF10-P50/Eco highlights the direct correlation between filler morphology and real-world thermal management capability.

The best-performing material was GF20-P25/Eco, which recorded the lowest LED surface temperature of 95.5 °C. The superior performance of this composite is attributed to two synergistic factors: increased GF loading (20 wt%) and optimal segregation structure enabled by 25 µm PMMA beads. The higher filler concentration contributed to the densification of the segregated network, while the structural organization provided by the PMMA template ensured continuity and uniform distribution. This combination yielded a thermal conductivity of 9.23 W/mK by far the highest among all tested materials—and directly translated into the most effective heat dissipation under LED operation.

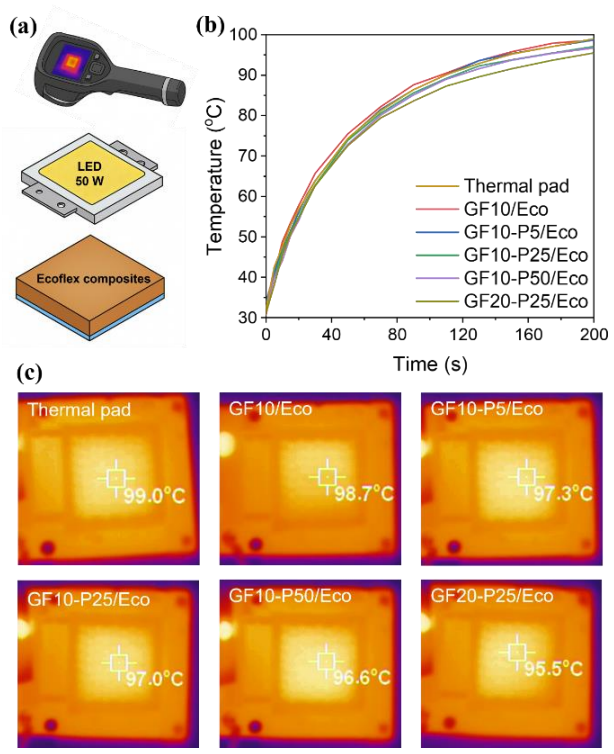

Figure 5. *(a) Heat dissipating experiment set up, (b) Temperature of LED surface using different Ecoflex composites and thermal pad, (c) Infrared images of LED surface at 200 s*

From a practical standpoint, the results of this experiment confirm that both filler content and segregation structure play decisive roles in determining the heat - spreading capability of flexible composites. The nearly 3.5 °C difference in LED temperature between the commercial thermal pad and GF20-P25/Eco, though seemingly small, is significant in thermal engineering, where even 1–2 °C of improvement can extend device lifetime, stabilize emission characteristics, and enable higher power operation without active cooling. Importantly, these improvements were achieved without compromising the mechanical compliance of the Ecoflex matrix, highlighting the potential of this strategy for wearable and flexible electronics where both softness and thermal functionality are required.

These results validate the utility of microstructural control via PMMA-induced segregation in maximizing the effectiveness of thermally conductive elastomers. The correlation between thermal conductivity and LED temperature reduction demonstrates the translation of intrinsic material properties into functional device-level benefits. The data further support the use of filler structuring as a more effective approach than random dispersion, even at the same filler loading, and provide a scalable design pathway for developing next-generation thermal interface materials with tunable performance.

4. Conclusion

This work presents a simple yet effective approach to fabricating thermally conductive, stretchable composites by inducing the segregation of GF within an Ecoflex matrix using PMMA beads as sacrificial templates. Through controlled variation of PMMA bead size and GF content, we demonstrated that a highly interconnected GF network can be formed at relatively low filler loading, significantly enhancing thermal conductivity while preserving mechanical compliance. Among all tested conditions, the use of 25 μm PMMA beads with 20 wt% GF (G20-P25/Eco) provided an optimal balance, achieving a thermal conductivity of 9.23 W/mK and elongation at break above 170%. Real-device tests with 50 W LEDs confirmed effective heat dissipation, with the LED surface temperature mounted on the GF20-P25/Eco composites reduced largely compared to the commercial thermal pad due to the high thermal conductivity and efficient heat transfer. This template-directed filler segregation strategy offers a scalable, solvent-free route for engineering multifunctional elastomers. The resulting composites exhibit excellent promise for thermal management in soft, wearable, and conformal electronic devices. These findings provide useful design insights for achieving simultaneous mechanical flexibility and thermal functionality in future generations of flexible electronics and soft robotics.

Acknowledgements: This research was funded by The Vietnamese Ministry of Education and Training under project number B2023.DNA.07.

REFERENCES

[1] M. C. Vu *et al.*, "Nacre-inspired nanocomposite papers of graphene fluoride integrated 3D aramid nanofibers towards heat-dissipating applications", *Chemical Engineering Journal*, vol. 429, p. 132182, 2022.

[2] S. Li *et al.*, "High thermal conductivity in cubic boron arsenide crystals", *Science (1979)*, vol. 361, no. 6402, pp. 579–581, 2018.

[3] J. Gu and K. Ruan, "Breaking Through Bottlenecks for Thermally Conductive Polymer Composites: A Perspective for Intrinsic Thermal Conductivity, Interfacial Thermal Resistance and Theoretics", *Nano-Micro Letters 2021 13:1*, vol. 13, no. 1, pp. 1–9, 2021.

[4] M. C. Vu, G. Park, Y. Bae, and S. Kim, "Enhanced Thermal Conductivity of Pressure Sensitive Adhesives Using Hybrid Fillers of SiC Microparticle and SiC Nanoparticle Grafted Graphene Oxide", *Polymer (Korea)*, vol. 40, no. 5, pp. 804–812, 2016.

[5] Y. H. Bae, M. J. Yu, M. C. Vu, W. K. Choi, and S. R. Kim, "Synergistic effects of segregated network by polymethylmethacrylate beads and sintering of copper nanoparticles on thermal and electrical properties of epoxy composites", *Compos Sci Technol*, vol. 155, pp. 144–150, 2018.

[6] H. Chen *et al.*, "Thermal conductivity of polymer-based composites: Fundamentals and applications", *Prog Polym Sci*, pp. 1–45, 2015

[7] N. Burger, A. Laachachi, M. Ferriol, M. Lutz, V. Toniazzo, and D. Ruch, "Review of thermal conductivity in composites: Mechanisms, parameters and theory", *Progress in Polymer Science*, vol. 61, pp. 1–28, 2016.

[8] D. K. Nguyen *et al.*, "Multilayered silver nanowires and graphene fluoride-based aramid nanofibers for excellent thermoconductive electromagnetic interference shielding materials with low-reflection", *Colloids Surf A Physicochem Eng Asp*, vol. 688, 2024.

[9] T. C. Nguyen, A. L. H. Pham, D. K. Nguyen, M. T. K. Lien, V. C. Nguyen, and M. C. Vu, "Ultrathin Aramid Nanofiber Composites with Alternating Multilayered Structure of Silver Nanowires and Boron Arsenide: Toward Superior Electrically Insulating Thermoconductive Electromagnetic Interference Shielding Materials", *ACS Appl Electron Mater*, vol. 6, no. 5, pp. 3704–3716.

[10] V. Cuong Nguyen *et al.*, "Layer-by-layer assembly of boron arsenide and copper nanoflake-based aramid nanofibers for thermoconductive electromagnetic interference shielding materials with superior mechanical flexibility and flame retardancy", *Journal of Industrial and Engineering Chemistry*, vol. 138, pp. 492-501, 2024.

[11] D. K. Nguyen *et al.*, "Ultratough and self-healable electromagnetic interference shielding materials with sandwiched silver nanowires in polyurethane composite films", *Polym Compos*, vol. 45, no. 16, pp. 14943-14952, 2024.

[12] D. K. Nguyen *et al.*, "Thermoconductive Graphene Fluoride Cross-Linked Aramid Nanofiber Composite Films with Enhanced Mechanical Flexibility and Flammable Retardancy for Thermal Management in Wearable Electronics", *ACS Appl Nano Mater*, vol. 7, no. 3, pp. 2724–2734, 2024.

[13] V. C. Doan, M. C. Vu, N. A. T. Thieu, M. A. Islam, P. J. Park, and S. R. Kim, "Copper flake-coated cellulose scaffold to construct segregated network for enhancing thermal conductivity of epoxy composites", *Compos B Eng*, vol. 165, pp. 772–778, 2019.

[14] M. Shtein, R. Nadiv, M. Buzaglo, K. Kahil, and O. Regev, "Thermally conductive graphene-polymer composites: Size, percolation, and synergy effects", *Chemistry of Materials*, vol. 27, no. 6, pp. 2100–2106, 2015.

[15] K. M. F. Shahil and A. A. Balandin, "Graphene-multilayer graphene nanocomposites as highly efficient thermal interface materials", *Nano Lett*, vol. 12, no. 2, pp. 861–867, 2012.

[16] V. C. Doan, M. C. Vu, M. A. Islam, and S. R. Kim, "Poly(methyl methacrylate)-functionalized reduced graphene oxide-based core–shell structured beads for thermally conductive epoxy composites", *J Appl Polym Sci*, vol. 136, no. 9, p. 47377, 2019.

[17] M. C. Vu, Q. V. Bach, D. D. Nguyen, T. S. Tran, and M. Goodarzi, "3D interconnected structure of poly(methyl methacrylate) microbeads coated with copper nanoparticles for highly thermal conductive epoxy composites", *Compos B Eng*, vol. 175, pp. 107105–107113, 2019.

[18] M. D. Bartlett *et al.*, "High thermal conductivity in soft elastomers with elongated liquid metal inclusions", *Proc Natl Acad Sci USA*, vol. 114, no. 9, pp. 2143–2148, 2017.

[19] D. Mani *et al.*, "3D structured graphene fluoride-based epoxy composites with high thermal conductivity and electrical insulation", *Compos Part A Appl Sci Manuf*, vol. 149, p. 106585, 2021.

[20] X. Wang and P. Wu, "Fluorinated Carbon Nanotube/Nanofibrillated Cellulose Composite Film with Enhanced Tough ness, Superior Thermal Conductivity, and Electrical Insulation", *ACS Appl Mater Interfaces*, vol. 10, no. 40, pp. 34311–34321, 2018.